DETERMINATION OF THE ROVING TRAJECTORIES FOR GENERIC AXYSYMMETRIC SHELLS OF REVOLUTION FABRICATED BY THE FILAMENT WINDING PROCESS

E. Vargas-Rojas[*], D. Chapelle, D. Perreux

Université de Franche-Comté, Institut FEMTO-ST, Département de Mécanique Appliquée, 24 Rue de l'Épitaphe, 25000 Besançon, France
*erikvargasrojas@hotmail.com

Keywords: curvature, filament winding, mandrel, non-geodesic, trajectory.

Abstract.

This research aims to develop a numerical tool which allows an integral design approach of generic shells of revolution intended for very high internal pressure applications, fabricated with the filament winding process. In order to define a generic winding model as a function of the winding angle, the stability conditions are stated for a generic case, and two axisymmetric geometries of revolution for the mandrel are proposed to validate the mathematical procedure: a convex and a concave geometry. Both shapes are described mathematically, so that the geodesic and the non-geodesic trajectories are defined and solved numerically. Experimental validation would be achieved by fabricating both geometries with a lathe type winder with five degrees of freedom. Wound shapes would be submitted to validation tests in order to control and to verify the correct placement of the roving. As a result the mathematical description of the filament winding process is achieved for two axysimmetric rotationally symmetric shapes.

1. Introduction

The development of hydrogen as an energy vector is related with renewable energy sources, such as hydraulic, sun or wind energy. Because of their intermittent nature, these energies must be stored so they can be used lately on demand. The energy that is not used immediately can be transformed to hydrogen by means of an electrolyser when considering renewable energy sources, or by the chemical reaction of the syngaz during the gasification process of the biomass. Producing hydrogen this way is one of the most efficient manners to store this kind of energy, allowing a subsequent use, with good performance [1].

The discharge pressures of the devices that transform the surplus energy to hydrogen go from atmospheric pressure up to 30 bars. In order to obtain reasonable storage volumes, hydrogen must be compressed, but compression itself is a process that consumes energy and that becomes less effective as the behavior of the gas differs to that of a perfect gas. So it is more effective and economic to store hydrogen directly from the device and to compress it up to 100 bars. This value is a compromise between the stored volume gain, and the consumed energy used for compression [1].

This project aims to continue the development of highly reliable storage tanks reinforced with composite materials, like for example type IV tanks for compressed hydrogen at 700 bar. Illustrated in figure 1, these composite tanks are fabricated using the filament winding process of carbon fiber over a polymer (thermoplastic) liner.

Figure 1. Type IV hydrogen storage tanks. Courtesy of MAHYTEC SARL.

Filament winding is a process in which continuous tows of strands are wound on a supporting form or mandrel [2]. Its best use is for making tube- and pipe-shaped objects. Since its introduction in the 60's, filament winding process has been used to develop filament-reinforced metal pressure vessels (type II and type III tanks), and metal-lined (type III) or plastic-lined (type IV) filament-wound pressure vessels (the latter consists of a very thin liner having minimum thickness required for impermeability and fabrication). Filament-wound structures are made using the polar, helical or hoop winding patterns. Polar winding is used to lay down fiber close to 0° with respect to the rotating axis, so roving generally passes close to or around the mandrel poles. Helical winding is used to deposit fiber at angles from 5° to 80° to the longitudinal axis. Hoop winding is used to lay down fiber close to 90° to the longitudinal axis.

The performance of type IV tanks depends on the materials used both for the liner and the reinforcement; on the failure and damage behavior under static, creep, or fatigue; and on the parameters comprised during the fabrication, such as the winding angles [3], the trajectories of the fiber [3, 4, 5], the tow tension [6], the winding speed [7], or the winding patterns [8, 9]. According to [3], geometry definition of a filament wound structure is one the aspects that has not been sufficiently treated using mathematical description. The theories supporting the complete manufacturing process are covered in the literature [2-10]; nevertheless there is still a lack of mathematical description methods from the design point of view. The scope of this article is to present the mathematical background that allows the definition of a generic winding model. In order to achieve this goal, a convex and a concave shell of revolution for the mandrel are studied in an effort to propose more complex shapes, rather than traditional cylinders, or semi-spheres. Both shapes are described mathematically, so that the geodesic and the non-geodesic trajectories can be defined and solved by means of numerical computing software.

Recent literature that has treated the mathematical definition of trajectories over a surface include: [3], as the study of the filament winding process itself; [5], as the study of overwrapped pressure vessels for hydrogen storage (type III) using aluminum liners; and [10], as the analysis of the elasto-plastic damageable behavior of composite laminates using filament wound pipes as test specimens.

2. Methodology
2.1 Geometrical description of mandrel

The chosen mathematical procedure requires that both the surface and the curve to be placed over it, to be derivable, in order to calculate their geometrical parameters [11, 12]. From this statement the surface **S** is continuous and regular, defined as a function of the meridian (θ) and parallel (φ) coordinates. For an axisymmetric mandrel, **S** is described according to the following equation expressed in spherical coordinates:

$$\mathbf{S} = \mathbf{S}(\varphi,\theta) = \{\rho(\theta)\sin(\theta)\cos(\varphi), \rho(\theta)\sin(\theta)\sin(\varphi), \rho(\theta)\cos(\theta)\} \tag{1}$$

On the other hand, the curve **C** to be traced over the surface is regular, continuous, of class C^2, and it is expressed as a function either of the arc length s (2), or of the independent parameters generating it (3):

$$\mathbf{C}(s) = \mathbf{C}(\varphi(s), \theta(s)) \tag{2}$$

$$\mathbf{C}(\theta) = \mathbf{C}\{x(\theta, \varphi(\theta)), y(\theta, \varphi(\theta)), z(\theta, \varphi(\theta))\} \tag{3}$$

The curve **C** has an orientation α with respect to the meridian of the surface, which means that the normal curvature will obtain two extreme values, i.e. the meridian k_m and parallel k_p curvatures when considering a shell of revolution. Normal curvature of **C**, expressed as a function of the orientation angle and the referred maximum and minimum principal curvatures is stated by (4):

$$k_n = k_m \cos^2 \alpha + k_p \sin^2 \alpha \tag{4}$$

Two axisymmetric geometries of revolution for the mandrel, whose contours are illustrated in figure 2, are proposed: a convex and a concave geometry with the origin of their radius traced at point m. The fulfillment of the complete procedure on these geometries should allow us to validate the mathematical approach.
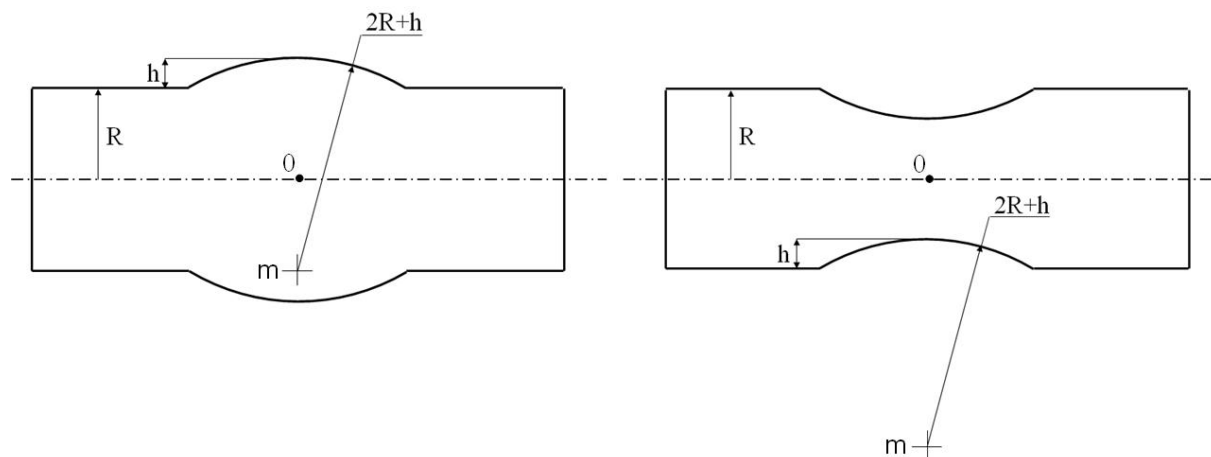

Figure 2. Convex-shaped mandrel and concave-shaped mandrel.

The discretized definition of the mandrel is given by equations (5) through (7): (5) for the cylinder, (6) for the convex shape, and (7) for concave geometry.

$$\rho_k = R / \sin(\theta_k) \tag{5}$$

$$\rho_k = \sqrt{L_1^2 + 3R^2 + R^2 \sin^2(\theta_k)} - R\sin(\theta_k) \tag{6}$$

$$\rho_k = \sqrt{L_1^2 + 4R^2 - 9R^2 \cos^2(\theta_k)} + 3R\sin(\theta_k) \tag{7}$$

Where ρ_k is the function parameter that defines the geometry in spherical coordinates (meridian angle, θ_k) with the origin of the spherical frame at point O (figure 2); R is the radius of the cylinder; and L_1 is the half-length either of the convex or concave shape.

2.2 Stability conditions of fiber placement.

The correct establishment of the stability condition of the fiber over the surface of the mandrel is a key to obtain the differential equation that defines the convenient curves over its surface. The stability of a trajectory depends of the relation between the lateral force, due to the change of the fiber angle α (or due to the shape of the mandrel); and the normal force, which depends on the longitudinal force F along the fiber. In the free-body diagram illustrated in figure 3, an orthonormal frame with origin at P is formed by the tangent **t**, normal **n**, and binormal **b** vectors.
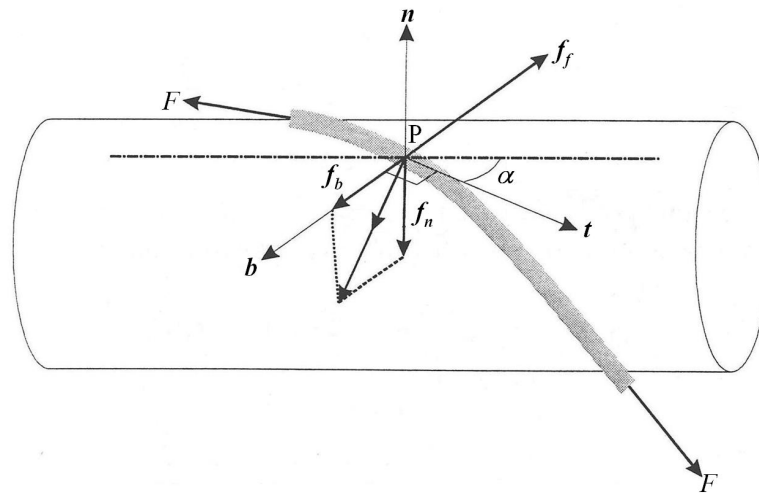

Figure 3. Forces developed along the fiber path [10].

It is assumed that the friction coefficient on the mandrel is μ and that μ^* is the real number parameter whose values belong to the interval [-μ, μ]. According to the friction theory, no slipping of the fiber occurs if the value of the lateral force f_b is lower than the product of the normal force f_n multiplied by the friction coefficient. This condition is defined by (8). As a direct consequence, and under the assumption of a local analysis, the previous relationship allows the description of a stable trajectory over the mandrel:

$$\mu \geq \frac{|f_b|}{|f_n|} \tag{8}$$

$$\mu^* = \frac{|f_b|}{|f_n|} \approx \frac{|F \cdot k_g|}{|F \cdot k_n|} = \frac{|k_g|}{|k_n|} \tag{9}$$

2.3 Mathematical procedure.

The chosen approach is based on the evaluation of the stability condition (9) considering the normal curvature as a function of the meridian and parallel curvatures, and on the solution of an ordinary differential equation (ODE) that describes the winding angle distribution. When the value of the normal curvature is zero, the geodesic curvature definition allows the integration of the Clairaut relation, as well as the evaluation of geodesic trajectories. The meridian and parallel curvatures are obtained as a function of geometrical parameters of the surface that are independent of the coordinate system, i.e. they are expressed as a function of E and G, that are the coefficients of the first fundamental form; and e and g that are the coefficients of the second fundamental form:

$$k_m = g/G \; ; \; k_p = e/E \tag{10}$$

Where:

$$E = \frac{dS}{d\varphi} \cdot \frac{dS}{d\varphi} \; ; G = \frac{dS}{d\theta} \cdot \frac{dS}{d\theta} \tag{11}$$

$$e = \frac{d}{d\varphi}\left(\frac{dS}{d\varphi}\right) \cdot \frac{\frac{dS}{d\theta} \times \frac{dS}{d\varphi}}{\left|\frac{dS}{d\theta} \times \frac{dS}{d\varphi}\right|} \; , g = \frac{d}{d\theta}\left(\frac{dS}{d\theta}\right) \cdot \frac{\frac{dS}{d\theta} \times \frac{dS}{d\varphi}}{\left|\frac{dS}{d\theta} \times \frac{dS}{d\varphi}\right|} \tag{12}$$

For a shell of revolution expressed in spherical coordinates, the said coefficients of the first fundamental become:

$$E = \rho_k^2 \sin^2\theta \; ; \; G = \rho_k^2 + (\rho_k')^2 \tag{13}$$

In consequence, the meridian and parallel curvatures can be expressed, respectively by:

$$k_m = \frac{2(\rho_k')^2 - \rho_k \rho_k'' + \rho_k^2}{\sqrt{\left(\rho_k^2 + (\rho_k')^2\right)^3}} \; , \; k_p = \frac{\rho_k \sin(\theta_k) - \rho_k' \cos(\theta_k)}{\rho_k \sin(\theta_k)\sqrt{\rho_k^2 + (\rho_k')^2}} \tag{14}$$

The ODE that defines the non-geodesic trajectories is obtained when evaluating (9) with (14) at (4), i.e. principal curvatures are replaced by the meridian and parallel ones:

$$\frac{d\alpha}{d\theta} = -\frac{1}{2}\frac{dE/d\theta}{E}\tan\alpha \pm \mu\left(\frac{\sqrt{G}}{\cos\alpha}\left(k_p \sin^2\alpha + k_m \cos^2\alpha\right)\right) \tag{15}$$

Differential equations that define the parametric coupling of θ and φ, and the length of the trajectory are expressed with (16) and (17), respectively:

$$\frac{d\varphi}{d\theta} = \sqrt{\frac{G}{E}}\tan\alpha \tag{16}$$

$$\frac{dL}{d\theta} = \frac{\sqrt{G}}{\cos\alpha} \tag{17}$$

2.4 Numerical resolution.

Considering its accuracy and stability, equation (15) is solved by the modified Euler Method, which is derived by applying the trapezoidal rule to the solution of $y' = f(x,y)$ [13]:

$$y_{n+1} = y_n + h\left(f\left(y_{n+1}, x_{n+1}\right) + f\left(y_n, x_n\right)\right)/2 \tag{14}$$

Where h is the step size, x is the independent coordinate, and y the dependent coordinate. Initial condition is $\alpha(0) \approx \pi/2$, i.e. fiber is placed lightly perpendicular to the generatrix lines at the beginning of the cylindrical part of the mandrel. Numerical differentiation of (5) through (7) as stated by (13) is achieved by the centered finite-difference method [14]. On the other side, numerical integration of (16) and (17) is made using the trapezoidal rule.

$$f'(x_i) = \left(-f(x_{i+2}) + 8f(x_{i+1}) - 8f(x_{i-1}) + f(x_{i-2})\right)/12h \tag{15}$$

$$f''(x_i) = \left(-f(x_{i+2}) + 16f(x_{i+1}) - 30f(x_i) + 16f(x_{i-1}) - f(x_{i-2})\right)/12h^2 \tag{16}$$

The numerical resolution of (15) is compared and validated with the respective analytical solution of the cylindrical part. In figure 4 the cylindrical mandrel geometry is depicted, as well as the distribution of α according to θ, φ according to the length of the mandrel z, and the length of the trajectory with respect to z. The same information is given for the convex- (figure 5), and the concave-shaped mandrels (figure 6).
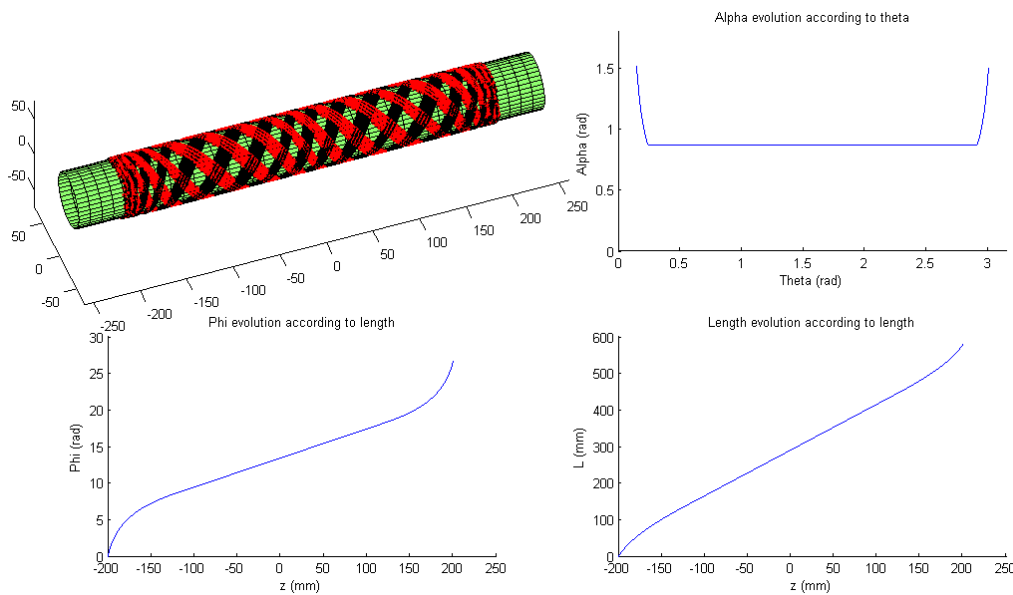

Figure 4. Numerical solution of the winding angle distribution for the cylindrical geometry.
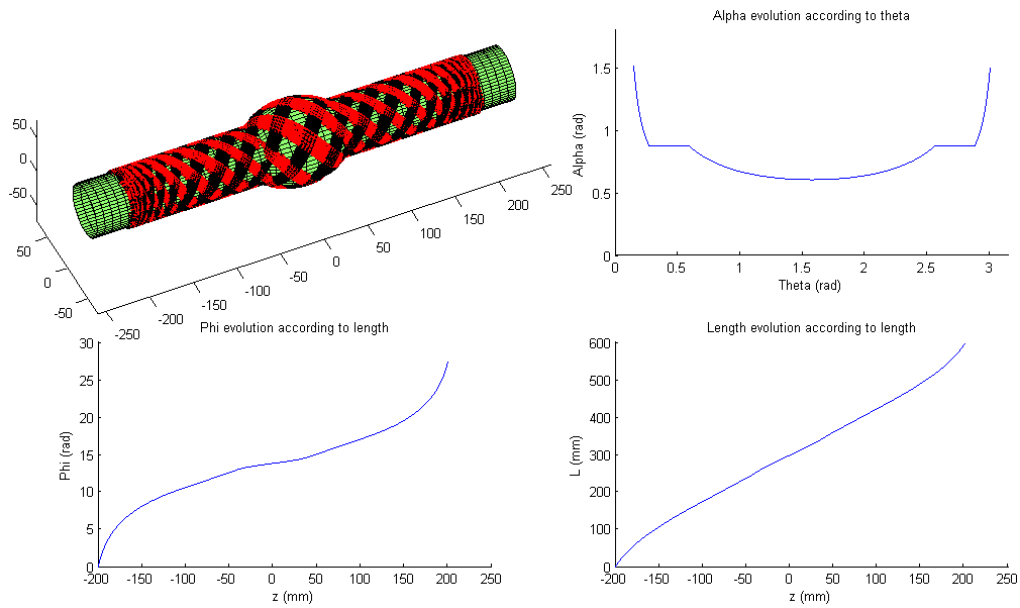
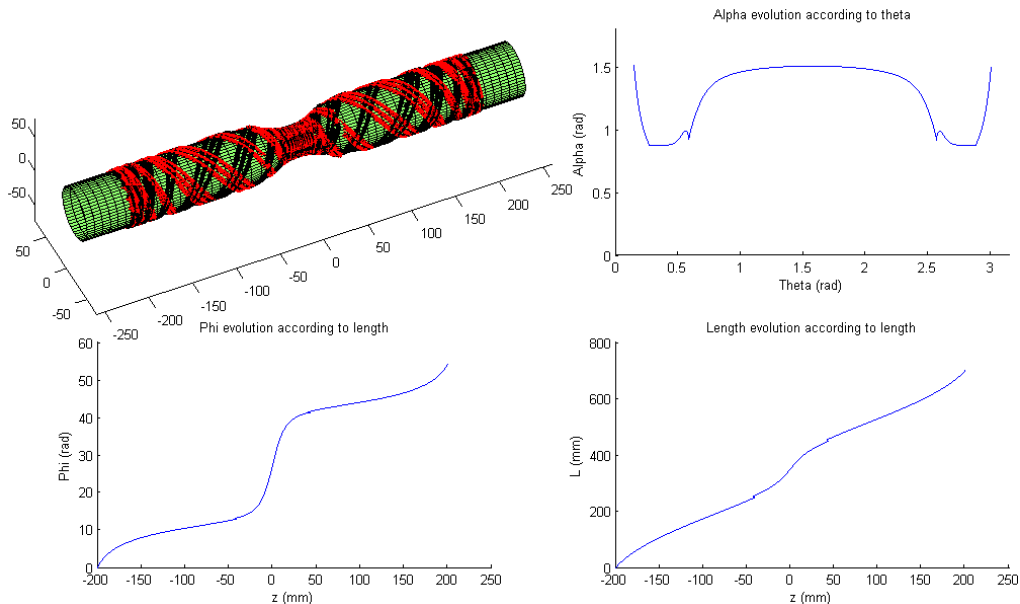**Figure 5**. Numerical solution of the winding angle distribution for the convex geometry.

Figure 6. Numerical solution of the winding angle distribution for the concave geometry.

3. Conclusions

The present paper paid attention on the description of the required methodology to ensure the overwrapping of a non-cylindrical mandrel by the filament winding manufacturing process. The mathematical background allowed the authors to establish the differential equation which permitted to obtain steady trajectories of the fiber over the surface of a mandrel with a complex geometry. Further analysis will let us to trace trajectories on the surface of the convex and concave mandrels already fabricated.

Acknowledgement

7

References

[1] Nardin. *Réservoirs de stockage d'hydrogène gazeux à pression modérée de type IV avec renfort en bio-composites totalement recyclables*. 19ème appel à projets ECOS Nord, formulaire de candidature. 2012.

[2] Shen. *A filament-wound structure technology overview. Materials and Physics* **42** (1995) 96-100.

[3] Koussios, Bersma, Beukers. *Filament winding. Part 1: determination of the wound body related parameters. Composites Part A* **35** (2004) 181–195.

[4] Gasquez, Chapelle, Thiebaud, Perreux, Colom, "*Etude et réalisation de la structure composite dans un réservoir d'hydrogène*". JNC 15, Marseille 6-8 juin 2007, p. 983-990, 2007.

[5] Gasquez. *Étude des réservoirs entièrement bobinés en composites destinés au stockage de l'hydrogène sous pression : cas des réservoirs type III*. Thèse présentée pour obtenir le grade de docteur de l'UFC. 2008.

[6] Mertiny, Ellyn. *Influence of the filament winding tension on physical and mechanical properties of reinforced composites. Composites Part A* **33** (2002) 1615-1622.

[7] Polini, Sorrentino. *Influence of winding speed and winding trajectory on tension in robotized filament winding of full section parts. Composites Science and Technology* **65** (2005) 1574-1581.

[8] Tarakcioglu, Samanci, Arikan, Akdemir. *The fatigue behavior of (±55°)₃ filament wound GRP pipes with a surface crack under internal pressure. Composite Structures* (2006).

[9] Rousseau, Perreux, Verdière. *The influence of winding patterns on damage behaviour of filament-wound pipes. Composites Sciences and Technology* **59** 9 (1999) 1439-1449.

[10] Lazuardi. *Une approche du rôle des contraintes internes liées a l'élaboration sur le comportement des composites stratifiés*. Thèse présentée pour obtenir le grade de docteur de l'UFC. (1998).

[11] Lischultz. *Differential Geometry*. Shaum Series. McGraw-Hill. New York. 1969.

[12] Kreyszig. *Differential Geometry*. Dover Publications. New York. 1959.

[13] Houcque. *Applications of Matlab: Ordinary Differential Equations*. 1-12. 2005.

[14] Chapra. *Applied numerical methods with Matlab*. Second Edition. McGraw Hill. 2005.